MD simulations of laser-induced ultrashort shock waves in nickel

Brian J. Demaske, Vasily V. Zhakhovsky, Nail Inogamov, Carter T. White, and Ivan I. Oleynik

Citation: AIP Conf. Proc. **1426**, 1163 (2012); doi: 10.1063/1.3686486
View online: http://dx.doi.org/10.1063/1.3686486
View Table of Contents: http://proceedings.aip.org/dbt/dbt.jsp?KEY=APCPCS&Volume=1426&Issue=1
Published by the American Institute of Physics.

MD SIMULATIONS OF LASER-INDUCED ULTRASHORT SHOCK WAVES IN NICKEL

Brian J. Demaske[*], Vasily V. Zhakhovsky[*], Nail A. Inogamov[†], Carter T. White[**] and Ivan I. Oleynik[*]

[*]*Department of Physics, University of South Florida, Tampa, FL 33620, USA*
[†]*Landau Institute for Theoretical Physics, RAS, Chernogolovka 142432, Russia*
[**]*Naval Research Laboratory, Washington, DC 20375, USA*

Abstract. The dynamics of ultrashort shock waves induced by femtosecond laser pulses were explored in nickel-glass and free-standing nickel films by molecular dynamics simulations. Ultrafast laser heating causes stress-confinement, which is characterized by formation of a strongly pressurized 100-nm-thick zone just below the surface of the film. For low-intensity laser pulses, only a single elastic shock wave was formed despite pressures several times greater than the experimental Hugoniot elastic limit. Because the material remains uniaxially compressed for < 50 ps, comparatively slow processes of dislocation formation are not activated. For high intensity laser pulses, the process of double wave breaking was observed with formation of split elastic and plastic shock waves. Presence of a trailing rarefaction wave acts to attenuate the plastic wave until it disappears. Agreement between the experimental and simulated Hugoniot was facilitated by a new EAM potential designed to simulate nickel in a wide range of pressures and temperatures.

Keywords: femtosecond laser, shock wave, molecular dynamics
PACS: 79.20.Eb, 62.50.Ef, 02.70.Ns

INTRODUCTION

Over the last several years, irradiation by ultrashort laser pulses has emerged as an efficient generator of shock waves with durations on the order of several tens to hundreds of picoseconds [1–4]. In particular, shock waves generated by femtosecond laser pulses, which have durations on the order of many atomic-scale processes, provide a unique opportunity to probe the response of materials to extreme conditions. A joint experimental [2] and computational [5] work investigated such ultrashort shock waves in thin aluminum films using femtosecond laser pulses with duration 150 ps. Results of these investigations indicated that the observed shock waves were most likely elastic despite amplitudes exceeding the commonly accepted value for the Hugoniot elastic limit (HEL) in metals ~ 1 GPa.

In another experimental work [1], shock waves were generated in thin nickel films deposited on glass by low-energy $0.2 - 0.5$ mJ femtosecond laser pulses with similar duration 130 fs. Making use of frequency-domain interferometry, precise measurements of the rear side response of the film upon arrival of the shock wave were obtained with subpicosecond resolution. As in the previous case, there were several indications, which will be discussed in detail later, that the observed shock waves were elastic. By performing complementary molecular dynamics simulations of nickel films on glass, the first of this two part work will address the structure of the shock waves observed in Ref. [1].

Because the driving laser pulse is transmitted through glass before being incident on the nickel film, there is a limit on the intensity of the pulses that can be used. Above this limit, optical breakdown of the glass occurs and the resultant plasma prevents any energy transmission to the metal surface. There-

Shock Compression of Condensed Matter - 2011
AIP Conf. Proc. 1426, 1163-1166 (2012); doi: 10.1063/1.3686486

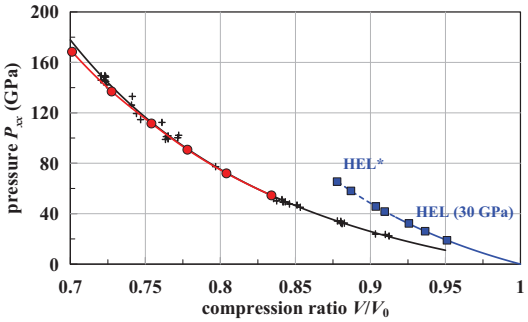

FIGURE 1. ~~(Color online)~~ $P-V$ Hugoniot for single-crystal~~line~~ Ni with SW propagation in the [110] direction. Squares are simulated points along the elastic branch and circles along the plastic branch. Crosses were taken from an experimental database [7]. ~~Position~~ of HEL corresponds to samples with a vacancy concentration of 0.1%. Dashed line gives the *metastable* extension of the elastic branch to HEL*.

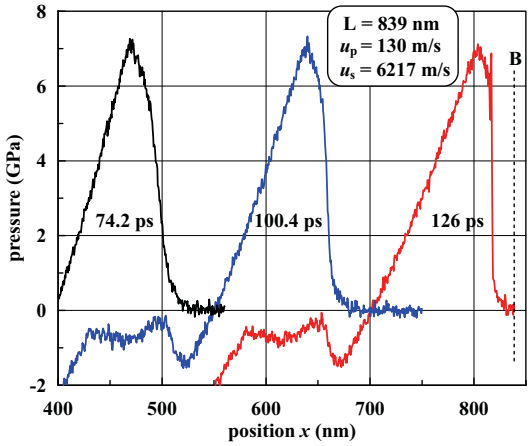

FIGURE 2. ~~(Color online)~~ Snapshots from molecular dynamics (MD) simulation of elastic wave propagating in [110] direction through 839 nm nickel film. The process of wave breaking takes a considerable amount of time and the shock front is not fully formed until reaching the edge of the sample.

fore, no experimental data for nickel from Ref. [1] were gathered for shock waves produced by high-intensity laser pulses. Once the glass substrate is removed, the driving pulse can be transmitted directly to the metal surface. By performing MD simulations of free nickel films in vacuum, the second part of this work will focus on the development and propagation of ultrashort shock waves induced by high-intensity femtosecond laser heating.

SIMULATION TECHNIQUE

Our simulations are directly related to the experiment reported in [1], where thin nickel films were deposited onto a $\sim 150\ \mu$m glass substrate. Single-crystalline nickel samples oriented in the [110] direction with a vacancy concentration of 0.1% deposited on a thin (~ 250 nm) layer of glass were simulated. To minimize the complexity of the calculations, the glass was approximated by the same nickel crystal with reduced density $\rho = 0.047\rho_{Ni}$ chosen so as to reproduce the acoustic impedance $Z = c_s\sqrt{\rho\rho_{Ni}}$ of glass, where c_s is the longitudinal sound speed of nickel in the [110] direction. Our simulations employed a new embedded atom method (EAM) interatomic potential for nickel specifically designed for use in wide ranges of pressures and temperatures [6]. Results from shock wave simulations are plotted in Fig. 1 against experimental data [7]. Good agreement along the plastic branch ensures that the new EAM potential accurately describes the response of nickel to shock compression.

In the first stage of heating, the femtosecond laser pulse transfers its energy to the conduction electrons within the skin layer (~ 10 nm). Within a time $\tau_{ie} \sim 10$ ps, the high-temperature electrons penetrate to a depth of d_T and thermalize with the surrounding cold ion subsystem. Since $\tau_{ie} < t_s$, where the acoustic time $t_s = d_T/c_s$, the heating is approximately isochoric, which leads to stress-confinement in a 100-nm-thick layer near the surface of the nickel film. The early stages, including laser energy deposition and electron-ion energy exchange, were simulated by a two-temperature hydrodynamics (2T-HD) code, which yielded the temperature distribution of the crystal after electron-ion thermalization. The 2T-HD temperature distribution was then fit to a one-dimensional Gaussian function $T(x)$. Using $T(x)$ as the target function for a Langevin thermostat that runs until τ_{ie}, the femtosecond laser heating was effectively reproduced in MD simulations. Different fluences were simulated by adjusting the maximum temperature at the film's surface $T(0)$. In addition, HD simulations were performed in which the nickel

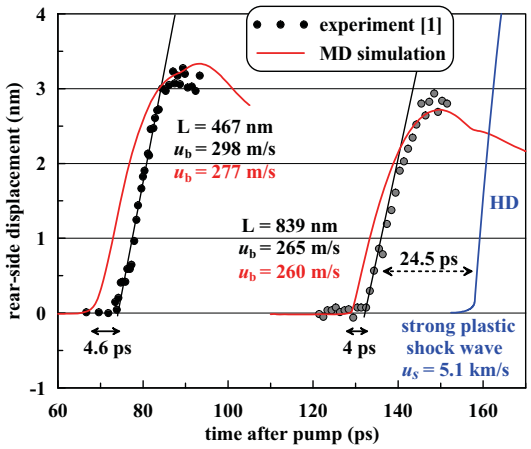

FIGURE 3. ~~(Color online)~~ Rear surface displacement upon arrival of shock wave for nickel films with thickness 467 nm and 839 nm. Circles are experimental points taken from [1]. Displacement profile of elastic shock wave and maximum surface velocity u_b from MD simulations coincide with experiment; whereas plastic shock wave simulated by HD does not. Experimental $u_b = 298$ m/s and $u_b = 265$ m/s were obtained from linear fits of experimental displacements immediately following shock arrival, see black straight lines.

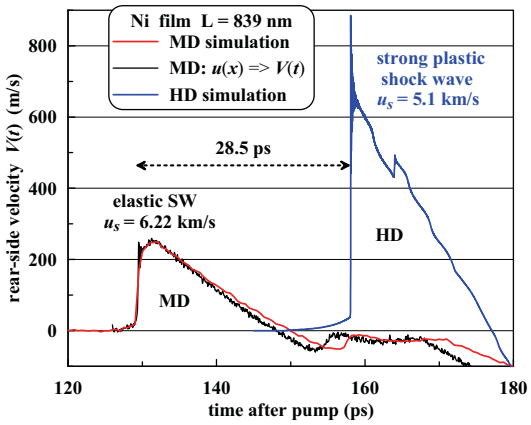

FIGURE 4. ~~(Color online)~~ Velocity of rear free surface upon arrival of elastic and plastic shock waves. High pressure plastic shock wave from HD simulation arrives significantly later than low pressure elastic shock wave simulated by MD.

sample is treated as a homogeneous (plastic) solid.

RESULTS AND DISCUSSION

As the stress-confined state decomposes, a strong compressive wave is formed, which propagates through the target. In our MD simulations, the compressive wave eventually broke into a weak elastic shock wave, as shown in Fig. 2. As is evident from the figure, the process of wave-breaking was relatively slow and a fully-formed shock front was only realized for the thickest (839 nm) film. The relative arrival times and rear side displacements of the shock waves from experiment and MD and HD simulations are shown in Fig. 3. Both experiment and MD give similar profiles and arrival times, whereas the strong plastic shock wave simulated by HD arrives significantly later and produces a much larger displacement. Simulated rear side velocities for an 839 nm film are shown in Fig. 4. Using the acoustic approximation, the simple transformation $u(x) \rightarrow V(t)$ applied to the MD simulation data, yields a velocity profile which agrees well with that directly obtained from the rear surface.

Two methods were used to measure the shock velocity u_s in experiment: in the first, an average value for $\overline{u_s}$ was directly measured from shock wave propagation times and, in the second, the maximum particle velocity u_p in the shock wave at the rear surface was measured and u_s was calculated from the plastic branch of the Hugoniot $u_s = 4.60 + 1.437u_p$. For a free surface, u_p is half of the maximum surface velocity $u_b = 2u_p$. The first method gives a value for $\overline{u_s}$ of 6.15 ± 0.39 km/s in 839 nm film, which is comparable to the MD result of 6.22 km/s; whereas the second method yields a significantly smaller shock velocity of 4.80 ± 0.02 km/s. Simulated and experimental values for u_p for two film thicknesses are given in Fig. 3. Experimental values for the maximum rear surface velocity, and by extension u_p, were obtained by linear fits to the rear side displacement data after shock wave arrival, shown in Fig. 3.

Agreement with MD results and the absence of shock wave splitting suggest that the waves observed in [1] are, in fact, purely elastic. In turn, this explains why the value for u_s obtained by the second method was significantly lower than that obtained by the first. It should be noted that attenuation of the relatively weak shock as it propagates through the sample has a small effect on the velocity measured at the rear

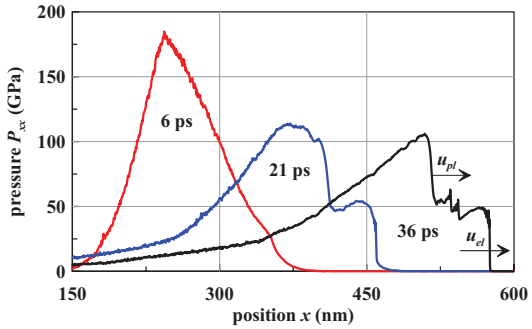

FIGURE 5. (Color online) Process of double wave breaking in 839 nm nickel film. Evolution of pressure P_{xx} profiles from initial strong compressive wave at 6 ps, to intermediate partially-formed elastic and plastic shock fronts at 21 ps, and fully-formed shock waves at 36 ps.

side, i.e. $\overline{u_s} \approx u_s$. Results obtained from HD simulations for a strong plastic shock wave show that a plastic wave with the same amplitude as the ones in experiment would have had a much smaller velocity than what was observed.

It is known that elastic-plastic transformations are not instantaneous, but require a finite amount of time τ_p. Thus, for compression times $t_c \ll \tau_p$, crystalline solids will respond elastically. In the limit of low stresses, τ_p can be inferred from Orowan's equation and, for copper, $\tau_p \approx 100$ ps [8]. By increasing the applied pressure, τ_p will decrease, yet should remain finite. Therefore, ultrashort shock waves can remain elastic as long as their amplitudes and widths are such that $t_c \ll \tau_p$. In experiment, the average compression time for ultrashort shock waves generated by femtosecond laser pulses is ~ 50 ps, hence such shock waves can be elastic as long as τ_p stays near 100 ps. Interestingly, such considerations do not distinguish a unique elastic limit. Even for shock amplitudes above HEL, we should expect a purely elastic response up to some limit. Indeed, our MD simulations indicate that ultrashort shock waves can exist in these *super-elastic* states. For example, $P_{HEL} \approx 30$ GPa for the simulated nickel films, yet we observed elastic shock waves with amplitudes > 45 GPa. By further increasing the applied pressure, we can expect the samples to plastically deform as τ_p falls below t_s.

We also performed MD simulations of nickel films in vacuum for a range of laser intensities and found that split elastic and plastic shock waves form for pressures > 50 GPa. The process of double wave-breaking is illustrated in Fig. 5. Due to the rarefaction tail, the plastic wave attenuated as it propagated through the sample. Once the amplitude of the plastic wave dropped below 50 GPa, then plastic deformation stopped and only an elastic wave remained. In principle, it is therefore possible to localize plastic deformation to a specific depth by simply adjusting the intensity of the incident laser pulse. This is similar to the observation in previous MD simulations of a localized polymorphic phase transition induced in a model diatomic molecular solid by hypervelocity impacts of ultra-thin flyer plates [9].

ACKNOWLEDGMENTS

This work was supported by ONR, NRL and NSF. N.A.I. was supported by the Russian Foundation for Basic Research. B.J.D. thanks APS GSCCM (D.S. Moore and M. Furnish), NNSA ASC (R.C. Little) and DTRA (S. Peiris) for travel support. Calculations were performed using NSF TeraGrid facilities, the USF Research Computing Cluster, and computational facilities of the Materials Simulation Laboratory at USF Physics Department.

REFERENCES

1. Gahagan, K. T., Moore, D. S., Funk, D. J., et al., *Phys. Rev. Lett.*, **85**, 3205–3208 (2000).
2. Ashitkov, S. I., Agranat, M. B., Kanel', G. I., et al. *JETP Lett.*, **92**, 516–520 (2010).
3. Armstrong, M. R., Crowhurst, J. C., Bastea, S., and Zaug, J. M., *J. Appl. Phys.*, **108**, 023511 (2010).
4. Whitley, V. H., McGrane, S. D., Eakins, D. E., et al., *J. Appl. Phys.*, **109**, 013505 (2011).
5. Zhakhovskii, V. V., and Inogamov, N. A., *JETP Lett.*, **92**, 521–526 (2010).
6. Demaske, B. J., Zhakhovsky, V. V., White, C. T., and Oleynik, I. I., AIP SCCM Conf. Proc. (2011).
7. Shock wave database: http://teos.ficp.ac.ru/rusbank/.
8. Loveridge-Smith, A., Allen, A., Belak, J., et al., *Phys. Rev. Lett.*, **86**, 2349–2352 (2001).
9. White, C. T., Robertson, D. H., and Brenner, D. W., *Physica A*, **188**, 357–366 (1992).